Hydration of Selected Divalent β″-Aluminas

G. S. Rohrer,* J. O. Thomas,† and G. C. Farrington

Department of Materials Science and Engineering, University of Pennsylvania, 3231 Walnut St., Philadelphia, Pennsylvania 19104

Received September 25, 1990. Revised Manuscript Received December 18, 1990

The absorption and desorption of H_2O by Ca(II)–β″-alumina, Ba(II)–β″-alumina, and Ba(II)–β″-ferrite were studied by thermogravimetry, differential scanning calorimetry, and evolved gas analysis, and the crystal structures of $Ba_{0.83}Mg_{0.67}Al_{10.33}O_{17}\cdot(H_2O)_{0.64}$ and $Ca_{0.83}Mg_{0.67}Al_{10.33}O_{17}\cdot(H_2O)_{1.0}$ were determined by the refinement of single-crystal X-ray diffraction data. The crystals are in the rhombohedral space group, $R\bar{3}m$, and have three formula units per hexagonal unit cell. The hexagonal cell dimensions for the hydrated Ba(II) isomorph area a = 5.617 (1) Å, c = 34.115 (8) Å, and V = 932.2 (4) Å^3, and for the hydrated Ca(II) isomorph are a = 5.628 (1) Å, c = 33.837 (11) Å, and V = 928.2 (4) Å^3. A comparison with previously reported data for other isomorphs indicates that in β″-alumina-type compounds absorbed water appears to interact more strongly with the structural framework than with the mobile cations.

Introduction

The ability of Na(I)–β″-alumina to undergo a wide variety of ion-exchange reactions is not only fascinating scientifically but of considerable practical importance for the low-temperature synthesis of metastable materials.[1] This nearly universal host structure also can absorb neutral molecules, such as water. In this sense, the β″-aluminas are similar to zeolites and clays. However, in the β″-alumina system, the availability of reasonably well-characterized single crystals and the ability to alter their chemical composition by ion exchange allows hydration reactions and their effects to be conveniently studied.

The reactions of various monovalent β″-aluminas with water have been studied by NMR and IR spectroscopy, X-ray diffraction, and thermal analysis.[2-5] Interest in the hydration of the monovalent isomorphs was stimulated by its effect on the stability of Na(I)–β″-alumina electrolytes used in high-energy density batteries. Somewhat less is known about the hydration of the divalent isomorphs, a class of compounds potentially applicable as optical materials.[6] A previous investigation from our laboratory provided the first experimental data on the reactivity of the divalent β″-aluminas with water,[7] and in several recent papers we have reported on the hydration reactions of Pb(II)- and Sn(II)–β″-alumina in considerable detail.[8-10] Here we report additional thermal analysis and structural data on the hydration reactions of Ca(II)- and Ba(II)–β″-alumina and compare these to the previously published results from the two post-transition-metal β″-aluminas to determine the degree to which the conduction-layer cation influences the hydration properties of the compound. To gauge the relative importance of the framework chemistry, we have also synthesized a new fast ion conductor, Ba(II)–β″-ferrite, and compared its water absorption reaction to that of Ba(II)–β″-alumina.

The exceptional ion-transport properties of Na(I)–β″-alumina originate in its unusual structure which consists of a rigid aluminum-magnesium oxide 'framework' and loosely-packed conduction layers in which the mobile cations and vacancies reside. The framework of Na(I)–β″-alumina is nearly the same for each isomorph. However, the arrangement of the mobile cations in the conduction layers varies in the different isomorphs. The most common cation sites are the Beevers–Ross-type (BR) sites, which are coordinated by four oxygen atoms, and the mid-oxygen (mO) sites, which are coordinated by six oxygen atoms. The structural parameters of interest in these nonstoichiometric compounds are the fractional occupancies of the sites and the degree of order between the cations and vacancies. In general, the arrangement of the cations in the conduction layer depends on their charge, size, and polarizability.

Previous studies have demonstrated that monovalent ions predominantly occupy BR sites and trivalent ions occupy mO sites, while divalent ions usually occupy a fraction of each. The precise distribution of divalent ions among the available sites has been investigated thoroughly by using single-crystal X-ray diffraction.[10,12-19] Several inconsistencies appear in the literature with regard to ion distributions, degree of cation vacancy order, and composition. Recently, it was proposed that the thermal history of a crystal influences the ionic arrangement in the conduction layer and that some of the inconsistencies could be accounted for in this way.[20] Some support for this

* To whom correspondence should be addressed at the Department of Metallurgical Engineering and Materials Science, Carnegie Mellon University, Pittsburgh, PA 15213.

† Institute of Chemistry, University of Uppsala, Box 531, S-751 21, Uppsala, Sweden.

(1) Sattar, S.; Ghosal, B.; Underwood, M. L.; Mertwoy, H.; Saltzberg, M. A.; Frydrych, W. S.; Rohrer, G. S.; Farrington, G. C. *J. Solid State Chem.* **1986**, *65*, 231.
(2) Kuhns, P. L.; Richter, L. J.; Conradi, M. S. *J. Chem. Phys.* **1982**, *76*, 6.
(3) Bates, J. B.; Wang, J. C.; Dudney, N. J.; Brundage, W. E. *Solid State Ionics* **1983**, *9/10*, 237.
(4) Larson, B. C.; Bates, J. B.; Dudney, N. J.; Barhorst, J. F. *Solid State Ionics* **1981**, *5*, 237.
(5) Garbarczyk, J.; Jakubowski, W.; Wasiucionek, M. *Solid State Ionics* **1983**, *9/10*, 249.
(6) Barrie, J. D.; Dunn, B.; Stafsudd, O. M.; Saltzberg, M. A.; Seshardi, R.; Farrington, G. C. *Solid State Ionics* **1988**, *28–30*, 344.
(7) Rohrer, G. S.; Farrington, G. C. *Mater. Res. Bull.* **1988**, *23*, 1747.
(8) Rohrer, G. S.; Farrington, G. C. *Chem. Mater.* **1989**, *1*, 438.
(9) Rohrer, G. S.; Farrington, G. C. *J. Solid State Chem.* **1990**, *85*, 299.
(10) Rohrer, G. S.; Thomas, J. O.; Farrington, G. C. *Chem. Mater.* **1990**, *2*, 395.
(11) Bettman, M.; Peters, C. R. *J. Phys. Chem.* **1969**, *73*, 1774.
(12) Thomas, J. O.; Alden, M.; Farrington, G. C. *Solid State Ionics* **1983**, *9/10*, 301.
(13) Boilot, J. P.; Colomban, P.; Lee, M. E.; Collin, G.; Comes, R. *Solid State Ionics* **1983**, *9/10*, 315.
(14) Thomas, J. O.; Alden, M.; Farrington, G. C. *Acta. Crystallogr.* **1984**, *C40*, 1763.
(15) Thomas, J. O.; Alden, M.; McIntyre, G. J.; Farrington, G. C. *Acta. Crystallogr.* **1984**, *B40*, 208.
(16) Carrillo-Cabrera, W.; Thomas, J. O.; Farrington, G. C. *Solid State Ionics* **1985**, *17*, 223.
(17) Alden, M.; Thomas, J. O.; Farrington, G. C. *Acta. Crystallogr.* **1985**, *C41*, 1700.
(18) Collin, G.; Boilot, J. P.; Colomban, P.; Comes, R. *Solid State Ionics* **1986**, *18/19*, 663.
(19) Saltzberg, M. A.; Thomas, J. O.; Farrington, G. C. *Chem. Mater.* **1989**, *1*, 19.

0897-4756/91/2803-0325$02.50/0

Table I. Summary of Ion-Exchange Reactions for β″-Ferrites

ion	ion radius, Å	exchange salt, wt %	temp, °C	atm	exchange time, h	comments
K(I)	1.33					as grown, a = 5.96 Å, c = 35.79 Å
Ca(II)	0.99	$^2/_3Ca(NO_3)_2$:$^1/_3CaCl_2$	485	air	14	partial exchange
Sr(II)	1.12	$^9/_{10}Sr(NO_3)_2$:$^1/_{10}SrCl_2$	600	air	11	full exchange, crystals etched
Ba(II)	1.34	$^2/_3Ba(NO_3)_2$:$^1/_3BaCl_2$	550	air	20	full exchange, a = 5.98 Å, c = 35.56 Å

suggestion was found in the results of an electron diffraction study that indicated that the arrangement of Eu(II) ions in Eu(II)–β″-alumina is dependent on the thermal history of a sample.[21] It has also been suggested that the intercalation of molecular metal oxide from the exchange salt during synthesis can result in the observed compositional variations.[13] However, an investigation of Pb(II)–β″-alumina found no evidence for the proposed intercalation of salt.[22] Our recent studies indicate that the apparent compositional and structural variations in the divalent β″-aluminas have likely been caused by the presence of undetermined quantities of water in the conduction layers of the crystal.

Experimental Procedures

The preparation of well-characterized single crystals of the divalent β″-aluminas has been discussed elsewhere.[1,23] However, the preparation of the alkaline-earth-metal β″-ferrites has not yet been reported and therefore is presented here. Single crystals of Cd(II)-stabilized K(I)–β″-ferrite were grown in a K_2O–KF–B_2O_3 flux following the experimental procedure described by Nariki et al.[24] This procedure produced thin, platelike crystals, the largest of which was about 3 mm in diameter in the 001 plane. Powder X-ray diffraction confirmed that the product was K(I)–β″-ferrite with refined lattice constants a = 5.957 (4) Å and c = 35.79 (3) Å, and energy-dispersive analysis of X-rays (EDAX) showed that the crystals contained Fe, Cd, and K. The composition of crystals grown by Nariki et al. using the same method was $K_{1.5}Cd_{0.8}Fe_{11}O_{17.8}$.[24] Preliminary impedance measurements demonstrated that the crystals were mixed electronic/ionic conductors.

The Na(I)–β″-ferrite samples were converted to Ba(II)–β″-ferrite by a method similar to that used to prepare the divalent β″-aluminas.[1,23] Approximately 100 mg of K(I)–β″-ferrite crystals were combined with approximately 10 g of an exchange salt ($^1/_3$ wt % $BaCl_2$:$^2/_3$ wt % $Ba(NO_3)_2$) in an alumina crucible. The combination was heated to 550 °C, at which point the exchange salt melted. After the exchange proceeded for 20 hours, the crucible was cooled to room temperature, and the exchange salt was dissolved away with warm water. When observed under the optical and scanning electron microscopes, the faces of the crystals parallel to the conduction layers were still smooth, but some etching was observed on the surfaces perpendicular to the conduction layers.

The small size of the crystals precluded the use of weight change and radiotracer techniques to assess the results of the ion exchange. However, EDAX detected barium in the crystals but no potassium, which indicated that the ion exchange was either complete or virtually so. The lattice parameters for this material, refined from the powder diffraction pattern, were a = 5.981 (2) Å and c = 35.56 (1) Å. Ca(II)- and Sr(II)–β″-ferrites were also synthesized, and the experimental conditions for these reactions are summarized in Table I.

Following ion exchange, samples were crushed with an alumina mortar and pestle and sieved to 40- and 150-μm powders for TG and DSC measurements. Single crystals of the Ca(II)- and Ba(II)–β″-alumina were selected from such powders for diffraction measurements. The experimental procedures used for the thermal analysis studies were identical with those used in the studies of the Pb(II)- and Sn(II)–β″-alumina isomorphs.[9,10] In each experiment the heating rate was 10 °C/min and the cooling rate was 0.5 °C/min.

Table II. Experimental Parameters for the Diffraction Studies

	Ca(II)	Ba(II)
abs coeff μ, cm^{-1}	13.3	36.5
transmission range	0.85–0.93	0.72–0.77
sin θ/λ_{max}, Å^{-1}	0.594	0.805
no. of indep reflns	1102	1157
R factor for equiv reflns	0.010	0.008
R factor for refinement on F_o^2	0.063	0.066
R factor for refinement on F_o	0.024	0.042
no. of reflns used ($>2\sigma(F^2)$)	962	1154
unit cell dimension a, Å	5.628 (1)	5.617 (1)
unit cell dimension c, Å	33.837 (4)	34.115 (8)
cell vol, Å^3	928.4 (2)	932.2 (4)

The diffraction measurements were performed on a Nonius CAD4 automatic four-circle X-ray diffractometer using graphite-monochromatized Mo Kα radiation. Preliminary studies of each crystal confirmed that the $R\bar{3}m$ space group of Na–β″-alumina was retained in these samples. Reflections were collected out to sin θ/λ = 0.805 and 0.594 Å^{-1} for the Ba(II) and Ca(II) compounds, respectively. The data were corrected for background, Lp effects, and absorption. The absorption correction was made using calculated absorption coefficients (36.5 and 13.3 cm^{-1} for the Ba(II) and Ca(II) compounds, respectively) and explicit descriptions of the crystals' morphology. The transmission factor for different reflections varied between 0.72 and 0.77 for the Ba(II) crystal and between 0.85 and 0.93 for the Ca(II) crystal. A number of reflections suspected to be affected by multiple reflection were eliminated from the data sets. Details of the diffration experiments are summarized in Table II. The refinement was based on minimizing the function $\sum w(F_o^2 - |F_c|^2)^2$, where the weighting function, w, is of the form $w = 1/\sigma^2(F_o^2)$, and $\sigma^2(F_o^2) = \sigma^2_{count}(F_o^2) + (kF_o^2)^2$, and k is an empirical constant set to 0.04. Reflections with $F_o^2 < 2\sigma(F_o^2)$ were not used in the refinements.

In the first step of each structure refinement, the observed Fourier synthesis was calculated by using a model that consisted of only the framework ions in their Na(I)–β″-alumina positions and a refined scale factor. Atomic positions were identified by plotting the Fourier synthesis for an area of the conduction layer, and, in later steps of the analysis, occupational, positional, and thermal parameters were refined. An oxygen atom was used to represent the H_2O molecule, and the hexagonal lattice parameters were determined by a separate least-squares refinement of at least 20 reflections. In addition, the occupations of adjacent BR sites in the same unit cell were refined independently, a procedure that has been demonstrated to improve the structural refinement of some divalent β″-aluminas.[15]

Results

Thermal Analysis. Figure 1a shows a thermogram for the hydration of Ca(II)–β″-alumina. The sample increased in weight by 2.85% while cooling from 400 to 150 °C at 0.5 °C/min. Figure 1b shows a thermogram for the dehydration reaction that occurred when the hydrated sample was heated in a dry gas. A 2.85% weight loss occurred between 200 and 350 °C, and the maximum rate of weight loss was at 300 °C. The mass spectrometer measured an increase in the partial pressure of water over the sample (Figure 1c) that was simultaneous with the weight loss. From these observations, it is reasonable to conclude that the increase in weight during cooling in a wet (partial

(20) Davies, P. K.; Petford, A.; O'Keefe, M. *Solid State Ionics* **1986**, *18*, 624.
(21) Saltzberg, M. A.; Davies, P. K.; Farrington, G. C. *Mater. Res. Bull.* **1986**, *21*, 1553.
(22) Tegenfeldt, J.; Underwood, M.; Farrington, G. C. *Solid State Ionics* **1986**, *18/19*, 668.
(23) Dunn, B.; Farrington, G. C. *Mater. Res. Bull.* **1980**, *15*, 1773.
(24) Nariki, S.; Ito, S.; Uchinokura, K.; Yoneda, N. *J. Cryst. Growth* **1987**, *85*, 483.

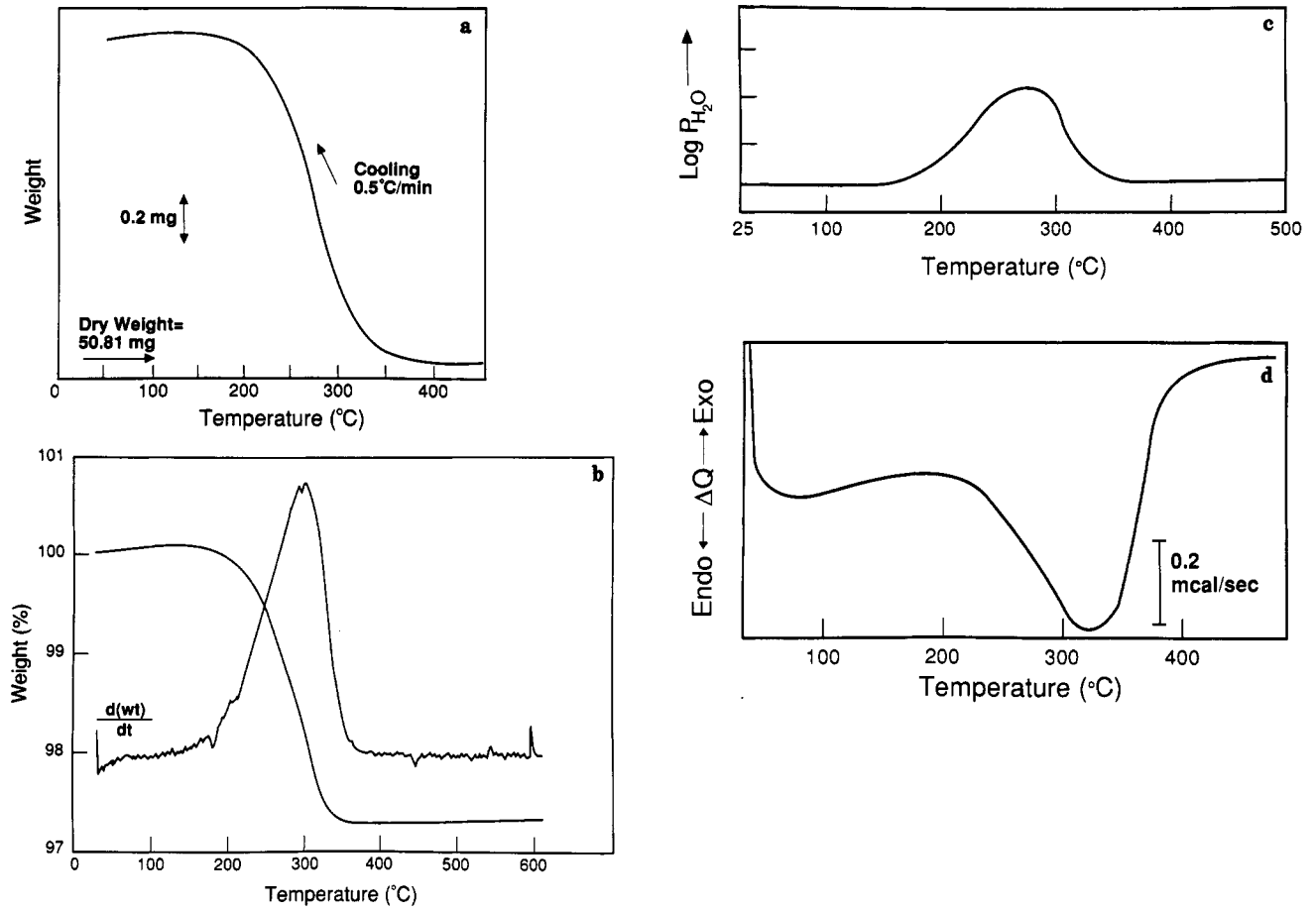

Figure 1. (a) Thermogram demonstrating that Ca(II)–β″-alumina hydrates when cooled slowly in a wet gas. (b) Thermogram showing the thermal decomposition of hydrated Ca(II)–β″-alumina. (c) Partial presssure of water over Ca(II)–β″-alumina during the dehydration reaction. (d) DSC trace of Ca(II)–β″-alumina showing an endothermic transition associated with the dehydration reaction.

pressure of water vapor approximately 20 mmHg) gas and the subsequent weight loss during heating in a dry gas were due to the absorption and desorption of water, respectively. From the measurement of the weight gain during cooling, the composition of the hydrated compound is calculated to be $Ca_{0.83}Mg_{0.67}Al_{10.33}O_{17}\cdot(H_2O)_{0.95}$.

Figure 1d shows the DSC trace for the dehydration of Ca(II)–β″-alumina at 10 °C/min in dry nitrogen. The endothermic transition observed during heating occurred at the same temperature as the weight loss and the increase in water vapor pressure discussed above and thus has been assigned to the desorption of water from the sample. By measurement of the area under the curve, the binding energy between the water and the lattice was estimated to be 0.81 eV/water molecule.

A Ba(II)–β″-alumina sample also increased in weight while cooling at 0.5 °C/min in wet N_2 from 375 to 200 °C (see Figure 2a). However, as the thermogram in Figure 2b clearly shows, two separate weight losses occurred during heating and not just one as with Ca(II)–β″-alumina. The first took place at approximately 250 °C and the second at 500 °C, with more than 90% of the weight being lost in the second transition. Figure 2c shows that an increase in the partial pressure of water vapor over the sample occurred simultaneously with the second weight loss. The amount of water evolved in the first step is apparently too small to be detected over the rather high background signal. Again, we conclude that the weight gain during cooling in a wet gas and the subsequent weight loss observed during heating in a dry gas were due to the absorption and desorption of water, respectively. In this case, the composition of the hydrated compound is $Ba_{0.83}Mg_{0.67}Al_{10.33}O_{17}\cdot(H_2O)_{0.62}$.

Figure 2d, a DSC trace for the decomposition of hydrated Ba(II)–β″-alumina, shows a weak endothermic transition centered at about 250 °C followed by a stronger one centered at about 500 °C. These peaks occur at the same temperatures as the weight losses and are therefore assigned to the enthalpy of dehydration. The binding energy for water, calculated by using the weight loss and heat evolution from both transitions, is 0.61 eV. Because the first transition is so weak, it is difficult to calculate an accurate enthalpy for this transition alone, and a calculation using the weight loss and heat evolution data from only the second transition gives approximately the same binding energy as the calculation using the combined data.

Figure 3a shows the hydration of a Ba(II)–β″-ferrite powder cooled at 0.5 °C/min in humid nitrogen. The weight gain on cooling indicates that the maximum water uptake was 0.16 water molecule/formula unit, one-fourth the amount of water absorbed by Ba(II)–β″-alumina. Figure 3b confirms that the weight lost on heating was equal to that gained on cooling, approximately 0.3 wt %, and shows that the dehydration temperature was 300 °C, about 200 °C less than that for Ba(II)–β″-alumina. Both the amount of water absorbed (under equivalent conditions) and the dehydration temperature differ substantially from what is observed with Ba(II)–β″-alumina.

Structure Analysis. The initial observed Fourier synthesis for the crystal with composition $Ca_{0.83}Mg_{0.67}Al_{10.33}O_{17}\cdot(H_2O)_{1.0}$ showed atoms at both the BR and off-axis 18h positions. A structural model was then refined in which Ca(II) ions were placed at the 18h positions, which lie along the conduction pathways between

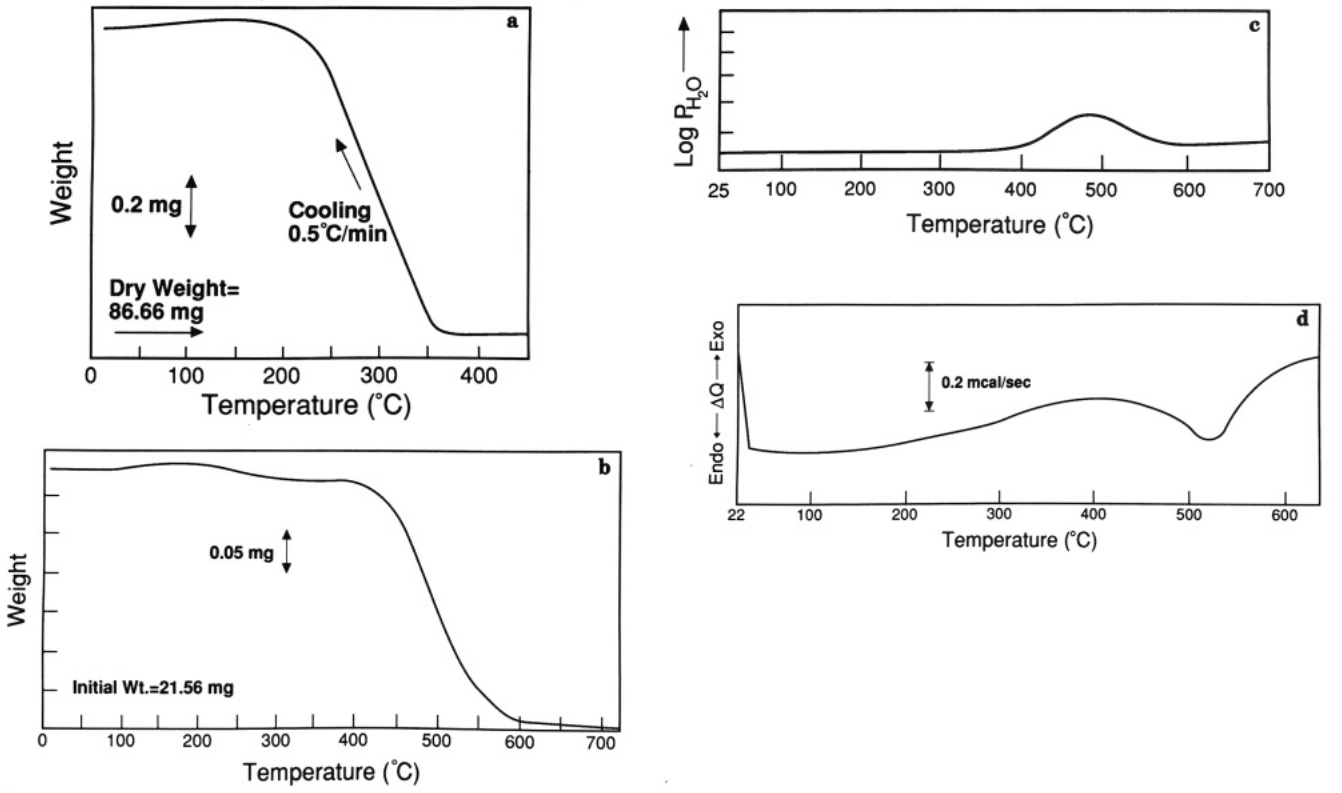

Figure 2. (a) Thermogram demonstraing that Ba(II)–β''-alumina hydrates when cooled slowly in a wet gas. (b) Thermogram showing the thermal decomposition of hydrated Ba(II)–β''-alumina. The dehydration occurs in two steps. (c) Partial pressure of water over Ba(II)–β''-alumina during the dehydration reaction. (d) DSC trace of Ba(II)–β''-alumina showing an endothermic transition associated with the dehydration reaction.

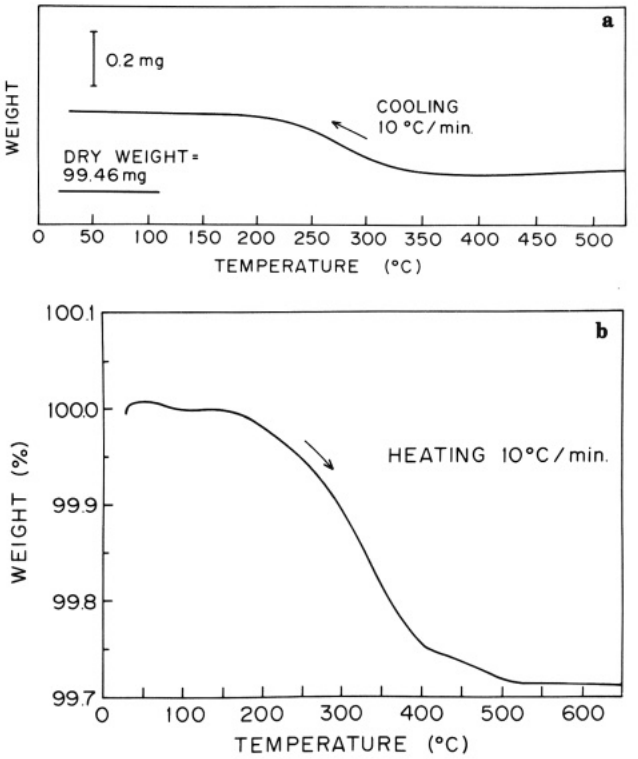

Figure 3. (a) Thermogram demonstrating that Ba(II)–β''-ferrite hydrates when cooled slowly in a wet gas. (b) Thermogram showing the thermal decomposition of hydrated Ba(II)–β''-ferrite.

Table III. Refined Atomic Positions and Occupancies for Hydrated Ca(II)–β''-Alumina

atom	x	y	z	occupation, %
Ca(1)	0.2220 (29)	0.1110 (14)	0.1668 (1)	31 (2)
Ca(1)′	−0.2220 (29)	−0.1111 (14)	−0.1668 (1)	43 (2)
OW(1)	0	0	0.1730 (2)	78 (1)
OW(1)′	0	0	−0.1730 (2)	41 (1)

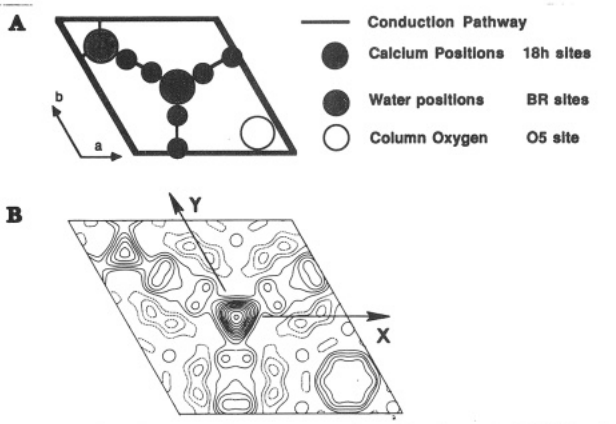

Figure 4. Conduction layer structure of hydrated Ca(II)–β''-alumina. (A) Schematic projection showing the conduction layer positions in hydrated Ca(II)–β''-alumina. (B) A section of the final observed Fourier synthesis at $z = {}^1/_6$ for hydrated Ca-(II)–β''-alumina calculated by using phases from the refined structural model. Levels are at 0.75 e/Å^3.

the mO and BR sites, and water molecules at the BR sites. Evidence for some substitutional disorder is indicated by the difference between the refined composition ($Ca_{0.75}Mg_{0.67}Al_{10.33}O_{17}\cdot(H_2O)_{1.2}$) and the known composition ($Ca_{0.83}Mg_{0.67}Al_{10.33}O_{17}\cdot(H_2O)_{1.0}$). The excess of water at the BR sites and the deficit of calcium at the 18 h sites indicates that calcium ions partially occupy the BR sites. The thermal model for the calcium ions involved β_{ij} terms, while both β_{ij} and γ_{ijk} terms were used for the thermal description of the water molecules. A selection of the refined atomic coordinates and occupancy factors are

Table IV. Refined Interatomic Distances in Hydrated Ca(II)-β″-Alumina

contact	multiplicity	dist, Å
Ca(1)–O(3)	1	2.601 (7)
Ca(I)–O(4)	2	2.715 (4)
Ca(1)–O(5)	2	2.866 (3)
OW(1)–O(3)	1	2.576 (8)
OW(1)–O(4)	3	2.645 (6)
OW(1)–O(5)	3	3.257 (1)
OW(1)–OW(1)′	3	3.277 (1)
OW(1)–Ca(1)′	1	2.178 (14)
OW(1)–Ca(1)′	2	3.911 (10)

Table V. Refined Atomic Positions and Occupancies for Hydrated Ba(II)-β″-Alumina

atom	x	y	z	occupation, %
Ba(1)	0	0	0.1697 (1)	80.3 (1)
Ba(1)′	0	0	–0.1697 (1)	2.9 (1)
OW(1)	0.1873 (33)	0.0963 (16)	0.1674 (5)	19.6 (1)

shown in Table III, and relevant interatomic distances are listed in Table IV. Figure 4 depicts the structure of the Ca(II)–β″-alumina conduction plane and the observed charge density distribution in the conduction layer.

The initial electron density maps showed that both the 18h and the BR sites were occupied in hydrated Ba(II)–β″-alumina, similar to the situation in Ca(II)–β″-alumina. However, in Ca(II) isomorph the 18h site is displaced 1.1 Å from the nearest BR site, while in Ba(II) isomorph the 18h site is only 0.91 Å away. The refinement of a model in which the Ba(II) ions are situated at BR sites and the water molecules occupy 18h sites indicated that the majority of the Ba(II) occupied only one of the two BR sites in the unit cell, leaving the BR′ site almost unoccupied and the 18h′ site completely unoccupied. Since simultaneous occupation of the 18h site and the BR site is forbidden, the total occupation of the two sites had to be constrained to 1.0 in later refinements. In addition, the total barium content was constrained to the known concentration, 0.83 ion/formula unit. The refinement of this model indicated that there were only 0.2 water molecule/formula unit, much less than the quantity determined from thermal analysis, which was 0.62. However, alternative structural models that gave similar agreement factors and predicted total water content more accurately had to be discarded because they predicted a number of physically unrealistic bond lengths. It is possible that the undetected water substitutionally occupies BR sites but is "masked" by the much greater scattering power of the Ba(II) ions that also reside there. The water at the 18h site was described with an isotropic thermal model, while both β_{ij} and γ_{ijk} terms were used in the thermal model for the barium at the BR sites. A selection of the atomic coordinates and occupancy factors is shown in Table V, and the relevant interatomic distances are lited in Table VI.

Discussion

Thermal Analysis. We chose to study Ba(II)– and Ca(II)–β″-aluminas to complement our earlier study of two post-transition-metal isomorphs, Pb(II)– and Sn(II)–β″-alumina, because these paired compositions have important similarities and differences. For example, Ba(II) and Ca(II) are both alkaline-earth-metal cations with a closed-shell configuration, while Pb(II) and Sn(II) are both group IV ions with the ns^2 outer-shell configuration. These four cations can naturally be divided into two groups on the basis of polarizability, the group IV cations being more polarizable than the alkaline-earth-metal cations. However, there are also differences within the two groups. For example, the ionic radius of Ba(II) is much larger than that of Ca(II), and the Sn(II) ion causes a large distortion in the β″-alumina framework and is highly localized at the BR site,[10] in contrast to the Pb(II) cation, which is distributed among several sites.[12] The ionic conductivity of Sn(II)–β″-alumina is also much lower than that of Pb(II)–β″-alumina. The comparison between these two isomorphs was discussed more completely in an earlier paper.[10]

Table VI. Refined Interatomic Distances in Hydrated Ba(II)-β″-Alumina

contact	multiplicity	dist, Å
Ba(1)–O(3)	1	2.541 (1)
Ba(1)–O(4)	3	2.768 (0)
Ba(1)–O(5)	3	3.245 (0)
OW(1)–O(3)	1	2.627 (1)
OW(1)–O(4)	2	2.719 (1)
OW(1)–O(5)	2	2.897 (0)
OW(1)–Ba(1)′	2	3.784 (1)

Table VII. Summary of Thermal Analysis Data

composition	% water by wt	binding energy, eV	dehydration temp, °C
Ca(II)–β″·$(H_2O)_{0.95}$	2.9	0.81	300
Sn(II)–β″·$(H_2O)_{0.74}$	2.0	0.75	300
Pb(II)–β″·$(H_2O)_{0.79}$			
overall	1.9	0.83	
first transition	1.25	0.79	215
second transition	0.67	0.90	380
Ba(II)–β″·$(H_2O)_{0.62}$			
overall	1.7	0.61	
first transition	0.13		250
second transition	1.57	0.60	500

The diversity of these four cations makes it interesting to compare and contrast their hydration and dehydration reactions (see Table VII). The compounds all hydrate readily, regardless of the mobile cation type. One difference is that Ba(II)– and Pb(II)–β″-alumina clearly dehydrate in two-step processes whereas Ca(II)– and Sn(II)–β″-aluminas dehydrate in single-step processes. Another differences is that Ba(II)–β″-alumina has a rather high dehydration temperature and low enthalpy of dehydration in comparison to the other three isomorphs, which are similar in these respects. There is no obvious correlation between the ion "types" discussed above and the reactivity of each isomorph with water. In fact, although some differences exist, the reactions are relatively insensitive to cation type. thus, we suggest that water molecules interact more strongly with the host lattice than with the mobile cations. If this is so, then the reactivity of the divalent β″-aluminas with water is a property of the entire family of materials, and the individual cations affect the hydration behavior in only secondary ways.

From this viewpoint, it is interesting to consider the predictions made by Garbarczyk et al.,[25] who considered that the hydration reactions of the β″-aluminas are influenced principally by the mobile cations. They presented a simple two-body model for the interactions between the mobile cations and the water molecules; interactions between the water molecules and the framework were completely ignored. Table VIII compares their predicted binding energies with those determined experimentally in this work and shows that the experimental values are generally lower. The predicted values are also very dependent on cation type, whereas the experimentally de-

(25) Garbarczyk, J.; Jakubowski, W.; Wasiucionek, M. *Solid State Ionics* **1986**, *18/19*, 653.

Table VIII. Comparison of Calculated and Experimental Binding Energies for the Divalent β″-Aluminas

mobile ion	binding energy,[a] eV	binding energy, eV
Ca(II)	2.69	0.81
Sr(II)	1.55	
Ba(II)	1.05	0.61
Pb(II)	1.51	0.83
Sn(II)		0.75

[a] Values calculated in ref 25 from two-body model.

termined values are much less sensitive to the identity of the cation. It seems clear from this comparison that the interaction between the mobile cations and water molecules is not the principal factor that determines the binding energy.

An intriguing aspect of the thermal analysis data is that Ba(II)–β″-alumina has both the highest dehydration temperature and the lowest binding energy for water. All things being equal, a reduced enthalpy of dehydration should result in a lower temperature of dehydration. Two factors may explain this apparent anomaly. The first concerns the number of 18h and BR sites available for occupation by water molecules. There are 3 times as many 18h sites as BR sites, and the configurational entropy of water molecules distributed on both 18h and BR sites would be higher than if the same molecules occupied only BR sites. The former is the case for the Ba(II) composition, while the latter appears to be true for Ca(II)–β″-alumina. This additional configurationl entropy would result in a reduced entropy difference between the water in the crystal and the water in the vapor, which in turn would lead to an increase in the thermal stability of hydrated Ba(II)–β″-alumina. It should be pointed out, however, that this extra source of entropy cannot alone account for the observed results.

A second factor to consider is that the "binding energies" quoted here were calculated from the enthalpy of dehydration measured for each compound. It was assumed that the enthalpy change of the mobile cation sublattice and the framework were only small components of the measured values, an assumption that is likely to be valid for the Ba(II) isomorph, since the lattice parameters and mobile cation arrangement are altered only slightly by hydration. This is in contrast to the Ca(II), Sn(II), and Pb(II) isomorphs, where dehydration leads to a significant alteration of the lattice parameters and mobile ion arrangement. Therefore, these factors are likely to make a greater contribution to the enthalpy of dehydration than in the case of the Ba(II) compound, an effect that would lead to an overestimation of the binding energies. Whatever the reason, the unusually high thermal stability of hydrated Ba(II)–β″-alumina is remarkable.

By comparing the data from the alkaline-earth-metal β″ isomorphs with previously published results on the post-transition-metal isomorphs, we have concluded that, for these compositions, the effect of cation type on hydration is secondary. The observation that the hydration properties of Ba(II)–β″-ferrite differ from those of Ba(II)–β″-alumina is consistent with this suggestion. If the Ba(II) cations determined the reactivity of the compound with water, then Ba(II)–β″-ferrite might have been expected to behave in much the same way as Ba(II)–β″-alumina. However, Ba(II)–β″-ferrite absorbs much less water than the alumina compound, which is consistent with a model in which water–framework interactions are the dominant factor in the hydration reactions.

Structure Analysis. The similar dehydration temperatures and enthalpies of the Ca(II) and Sn(II) isomorphs suggest that water molecules are bound by a similar mechanism in each crystal. Theoretically, the minimum distance between a water molecule and a mobile ion in Ca(II)–β″-alumina would be 2.18 Å, which corresponds to a water molecule in a BR site and a Ca(II) in an adjacent 18h site. However, this distance is shorter than the sum of the ionic radii of oxygen and calcium (2.33 Å) and much shorter than typical calcium–water separations in zeolitic materials, which vary from 2.41 to 2.64 Å.[31] Therefore, it is unlikely that this configuration actually occurs. The next possible interatomic separation is 3.91 Å, which implies a much weaker interaction between the calcium ion and the water molecule. Similarly, the closest approach betwen a water molecule and a Sn(II) ion in the conduction layer is 3.12 Å.[10] The location of the water molecule in the framework and its position with respect to the mobile cations indicates that the interaction between the two is weak and that it is primarily the water–framework interaction that determines the dehydration characteristics.

Table IX. Cell Dimensions for Hydrated and Anhydrous Divalent β″-Aluminas

compound	a, Å	c, Å	cell vol, Å^3
Ca(II)–β″-Al_2O_3 (ref 14)	5.613 (1)	33.270 (5)	907.8 (3)
Ca(II)–β″-Al_2O_3·$(H_2O)_{1.0}$	5.628 (1)	33.837 (4)	928.4 (2)
Ba(II)–β″-Al_2O_3 (ref 15)	5.619 (1)	34.084 (20)	932.0 (7)
Ba(II)–β″-Al_2O_3·$(H_2O)_{0.64}$	5.617 (1)	34.115 (8)	932.2 (4)
Sn(II)–β″-Al_2O_3 (ref 10)	5.6206 (5)	34.311 (7)	936.8 (3)
Sn(II)–β″-Al_2O_3·$(H_2O)_{0.74}$	5.623 (1)	34.191 (11)	930.5 (4)
Pb(II)–β″-Al_2O_3 (ref 12)	5.610 (1)	33.97 91)	925.8
Pb(II)–β″-Al_2O_3·$(H_2O)_{0.86}$	5.608 (3)	34.124 (8)	930.5 (4)

The structural results for the Ba(II) isomorph indicate that essentially all of the Ba(II) ions reside in the BR sites, and there is a very low probability of nearest-neighbor BR site occupation, a conclusion that agrees with earlier studies.[15] Water, on the other hand, occupies either BR sites or 18h sites that are only slightly displaced from the BR site (0.9 Å), an arrangement similar to the placement of the water in the hydrated Sn(II) and Ca(II) isomorphs. This structure also implies that the water does not directly coordinate with the Ba(II) cation, again a situation similar to that for the Sn(II) and Ca(II) isomorphs. According to our structural model, the closest possible distance between a water and a Ba(II) ion is 3.78 Å, a situation that occurs only for cations in the BR′ site (roughly 4%). More frequently, the Ba(II) is separated from the water by 4.9 Å, nearly a unit cell dimension.

It is interesting to compare the structures of these hydrated compounds to the structures of their anhydrous forms, keeping in mind that earlier results on so-called "anhydrous" compounds were obtained from crystals that had been exposed to air and certainly were somewhat hydrated, though not to the extent of those used in this study. Partial hydration may explain why the refined concentration of mobile cations was often higher than expected (for example, see ref 14) and varied from crystal to crystal (for example, compare refs 12 and 18).

Hydration changes the unit cell dimensions: in Ca(II)–, Pb(II)–, and Ba(II)–β″-alumina, the length of the c axis increases upon hydration, while in Sn(II)–β″-alumina it decreases. Lattice paramter data are summarized in Table IX. The c-axis length decreases in Sn(II)–β″-alumina because of a rearrangement of the conduction layer cations,[10] and the c-axis length increases in the other isomorphs because the water molecules "prop" open the conduction layers. The cell parameter of the Ba(II) isomorph changes very little, presumably because the large Ba(II) ions have already expanded the lattice. Conversely, the cell dimension of the Ca(II) isomorph increases the most, because the smaller calcium ions do not themselves prop open the space between the conduction layers.

Hydration can also alter the arrangement of ions in the conduction layers of the divalent β″-aluminas. For example, an earlier study of Ca(II)–β″-alumina indicated that the calcium ions reside at BR and mO sites,[14] but in the hydrated compound the ions prefer the 18h sites. The case is similar for Sn(II)–β″-alumina, in which the ions occupy only the BR sites in the anhydrous compound but predominantly occupy the $(2x, x, -z)$ sites in the hydrated compound.[10] In both of these cases, the water molecule displaces the mobile cation from the BR site and therefore dramatically alters the structure of the conduction layer. However, hydration does not significantly alter the ion arrangement in the Ba(II) isomorph, and the Ba(II) ions preferentially occupy the BR site in both the hydrated and the anhydrous compound. The reason water displaces Ca(II) and Sn(II) off the BR sites but not Ba(II) is probably related to the size of the Ba(II) ion and the size of the available sites in the β″-alumina framework. It is possible that while the Sn(II) and Ca(II) ions can occupy other conduction layer positions, steric factors prevent the larger Ba(II) (ionic radius = 1.34 Å) ion from moving away from the BR site, which is the largest available site in the framework.

Effect of Hydration on Physical Properties. Phase transformations that are dependent on thermal history have been detected calorimetrically in the divalent β″-aluminas.[26-28] Because samples cooled very slowly or annealed at temperatures between 100 and 300 °C exhibited endothermic peaks in the heat capacity, while those quenched to room temperature did not, these peaks were interpretted as signs of thermal-history-dependent solid-state phase transformations or order/disorder transformations. A dehydration reaction was not considered as a possible explanation for the observed transition, since precautions had been taken to maintain anhydrous conditions. We now know that these compounds are extremely hygroscopic and that powdered samples hydrate under the conditions used in the calorimetric experiments.[8] The phase transformations detected in these experiments were actually the dehydration reactions of the partially hydrated compounds.

Hydration also effects the optical and electrical properties of the β″-aluminas. In some cases, the ionic conductivity[9] and optical fluorescence[10,29] of these materials are drastically reduced. In addition, the vacuum dehydration of Pb(II)- and Sn(II)–β″-alumina creates a population of defects that has strong optical absorption bands in the visible range and brings about an insulator-to-semiconductor transition.[8] The effects of these hydration-related phenomena on the physical properties of these materials must be considered in the design of optical and electrical devices that incorporate them.

Comparison with Other Hydrated Inorganic Solids. Because water interacts with many other inorganic compounds in a variety of ways, it is interesting to consider our results in a broader context by comparing them to other oxides. First, there are the monovalent and trivalent isomorphs of β″-alumina, which also hydrate. For example, Na(I)–β″-alumina hydrates to the composition $Na_{1.67}Mg_{0.67}Al_{10.33}O_{17}\cdot(H_2O)_{0.4}$[30] and Nd(III)–β″-alumina hydrates to the composition $Nd_{0.56}Mg_{0.67}Al_{10.33}O_{17}\cdot(H_2O)_{0.7}$.[31] Two values for the binding energy of water in Na(I)–β″-alumina found in the literature, 0.58[30] and 0.78 eV,[5] do not differ substantially from those found for the divalent isomorphs. Although a binding energy for water in the Nd(III) isomorph has not yet been reported, we expect that it would be comparable to that of the other isomorphs. In any case, hydration is a characteristic of the entire β″-alumina family.

The β″-gallates and β″-ferrites are isomorphic with β″-aluminas, except that the framework Al(III) is substituted by Ga(III) or Fe(III), respectively. In general, it has been observed that the gallates hydrate much more readily than the aluminas.[32] The only available result for the β″-ferrites, that presented here, indicates that the ferrite lattice is less hygroscopic than the alumina lattice. The similarities among the alumina isomorphs and the variations in behavior of the gallates, ferrites, and aluminas support the earlier proposal that the β″ framework has a stronger influence on the hydration reaction than the mobile cation. The tendency for hydration appears to be greatest in the gallates, less in the aluminates, and even less in the ferrites.

The β″ family should be categorized with the clays and zeolites as a zeolitic-type material, which is distinguished from a stoichiometric hydrate by its ability to absorb or desorb water from its structure without any significant alteration to the crystal lattice. The zeolites, like the β″ compounds, readily undergo ion exchange, and the effect of mobile cation type on hydration has been studied. The binding energy of water in various divalent ion-exchanged zeolites can be calculated from existing calorimetric data.[33,34] In Ba(II)- and Ca(II)-exchanged zeolites X and Y, the binding energies for water vary from 0.67 to 0.75 eV/water molecule, energies not unlike those found for the divalent β″-aluminas. However, X-ray diffraction data have led to the conclusion that zeolitic water directly coordinates the mobile cations rather than the framework.[34] Considering the similarity of the binding energy for water in zeolites and β″-aluminas, it is interesting to note that the hydrated zeolites are much less stable than the hydrates β″-aluminas; thermal analysis data show that divalent ion exchanged zeolite A dehydrates below 200 °C.[33]

The surface of γ-alumina, which is structurally similar to a β″-alumina conduction plane but without the mobile cations, can absorb a monolayer of water. Most of the water on this surface is stored as hydroxyl groups, which condense to water and leave the surface when heated.[35] The heat of adsorption of water vapor for this surface is 0.65–0.95 eV.[35] The similarity of these energies with the dehydration enthalpies of the divalent β″-aluminas suggests the possibility that water also may be stored in the β″-alumina lattice as hydroxyl groups, a proposition that can account for the similar behavior of the β″-aluminas with respect to water and the unusual stability of water in the Pb(II) and Ba(II) isomorphs. However, it is not possible to distinguish between molecular water or hydroxyl water on the basis of the results presented here.

Conclusions

The results of our thermal and structural study of two alkaline-earth-metal β″-alumina compounds, when compared to earlier results from two post-transition-metal β″-aluminas, indicate that water most strongly interacts

(26) Garzon, F. H.; Davies, P. K. *Solid State Ionics* **1988**, *28-30*, 377.
(27) Rohrer, G. S.; Davies, P. K.; Farrington, G. C. *Solid State Ionics* **1988**, *28-30*, 354.
(28) Saltzberg, M. A.; Garzon, F. H.; Davies, P. K.; Farrington, G. C. *Solid State Ionics* **1988**, *28-30*, 386.
(29) Saltzberg, M. A. Ph.D. Thesis, University of Pennsylvania, 1988.
(30) Dudney, N. J.; Bates, J. B. *J. Am. Ceram. Soc.* **1987**, *70*, 816.
(31) Queenan, R. Ph.D. Thesis, University of Pennsylvania, 1989.
(32) Foster, L. M.; Arbach, G. V. *J. Electrochem. Soc.* **1977**, *124*, 104.
(33) Coughlan, B.; Carroll, W. *J. Chem. Soc., Faraday Trans. 1* **1976**, *72*, 2016.
(34) Barrer, R. M. *Zeolites and Clay Minerals as Sorbents and Molecular Sieves*; Academic Press: New York, 1978.
(35) Peri, J. B. *J. Phys. Chem.* **1965**, *69*, 311.

with the β''-alumina framework and not with the mobile cations. In some cases, partial hydration of the divalent β''-aluminas is quite difficult to avoid and can have dramatic effects on the structural, electrical, and optical properties of the compounds. In addition to these measurements on the aluminas, we have also synthesized several β''-ferrites for the first time. A comparison of the hydration reactions of Ba(II)-β''-ferrite and Ba(II)-β''-alumina suggests that the β''-ferrite lattice is less hygroscopic than the β''-alumina lattice.

Acknowledgment. This research was supported in Sweden by the Natural Science Research Council (NFR) and, in the United States, by the Office of Naval Research. Additional support by the National Science Foundation, Materials Research Laboratory Program, under Grant No. DMR-8519059, is gratefully acknowleged.

Registry No. $K_{1.5}Cd_{0.8}Fe_{11}O_{17.8}$, 132232-90-7; $Ba_{0.83}Mg_{0.67}Al_{10.33}O_{17}\cdot(H_2O)_{0.62}$, 119356-38-6; $Ca_{0.83}Mg_{0.67}Al_{10.33}O_{17}\cdot(H_2O)$, 132259-23-5; $BaCl_2$, 10361-37-2; $Ba(NO_3)_2$, 10022-31-8; $Ca(NO_3)_2$, 10124-37-5; $CaCl_2$, 10043-52-4; $Sr(NO_3)_2$, 10042-76-9; $SrCl_2$, 10476-85-4.

Supplementary Material Available: A listing of interatomic distances, atomic positions, and structure factor amplitudes (32 pages). Ordering information given on any current masthead page.

Topological and Geometrical Characterization of Sites in Silicon Carbide Polytypes

Michael O'Keeffe

Department of Chemistry, Arizona State University, Tempe, Arizona 85287

Received October 2, 1990. Revised Manuscript Received January 16, 1991

Sites in SiC polytypes are classified by the numbers of neighbors they have. It is shown that classification by numbers of geometrical neighbors and by numbers of topological neighbors leads to identical results, with the topological description leading to a convenient label for the type of site. The type of site in a layer depends only on the type (h or c) of neighboring layers and not on the type of the layer itself. Ideal coordinates and identification of sites are given for a number of simpler polytypes. A possible application to Si NMR is indicated.

Introduction

Considerable interest is attached to the phenomenon of polytypism in compounds. The SiC polytypes in particular have been intensively investigated because of their valuable physical properties. The question of why particular polytypes occur is a subject of intensive study,[1] but that topic is not addressed here. However, recent applications[2,3] of MASS NMR have focused attention on identifying the different types of site in these crystals. The problem is also of interest to ESR studies[4] and presumably to other spectroscopies also. This paper takes a predominantly topological approach to this problem and presents a new classification of types of site in polytypes with structures based on the principle of closest-sphere packings. Definitions and terminology relevant to the naming of polytypes are to be found in the monograph by Verma and Krishna[5] and in a recent International Union of Crystallography report.[6]

It should be emphasized that the purpose of this paper is to propose a concise and exact notation for different kinds of site; something which, to my knowledge, has not been done fully before. Reference to physical measurements, in particular NMR spectroscopy, is solely in the context of comparison with other systems of identifying different kinds of site, although it is believed that the system of classifying sites presented here will ultimately prove useful in this and other spectroscopic contexts.

In the closest packing of spheres,[5] the structure can always be described in terms of a hexagonal cell. The atoms lie on 3^6 layers centered over one of $0,0,z$, $^1/_3,^2/_3,z$, or $^2/_3,^1/_3,z$. These three positions are conventionally labeled A, B, and C. Stacking of layers in close packing is customarily denoted by a sequence of symbols c and h. An h layer is one that has the same symbol (A, B, or C) for the layers above and below; a c layer has different symbols for the layers above and below. The two simplest examples are cubic close packing (c = ABCABC...) and hexagonal close packing (h = ABAB...). As is well-known, as far as first and second neighbors are concerned, the h and c packings have the same numbers of neighbors although their arrangement in space is different. They differ however in numbers of further neighbors. Thus h has 2 and 18 neighbors at distances of $\sqrt{8/3}$ and $\sqrt{3}$ times the nearest-neighbor distance, whereas the corresponding numbers for c are 0 and 24.

In more complex polytypes of closest packing there will be a number of distinct types of site according to whether an atom in the layer and its neighboring layers is c or h. To take an example, the sphere packing ABCACB... can be symbolized hcc. The A layers are h, and the B and C layers (which are related by symmetry) are c. There are thus two distinct types of site. If one examines the *numbers* and *distances* of neighbors of an atom in the h layer,

(1) Heine, V.; Cheng, C. In *From Geometry to Thermodynamics: Common Problems of Quasicrystals, Liquid Crystals and Incommensurate Insulators*; (Toledano, J.-C., Ed.; Plenum: New York, 1990.
(2) Guth, J. R.; Petusky, W. T. *J. Phys. Chem.* **1987**, *91*, 5361.
(3) Hartman, J. S.; Richardson, M. F.; Scheriff, B. L.; Winsborrow, B. G. *J. Am. Chem. Soc.* **1987**, *109*, 6059.
(4) Woodbury, H. H.; Ludwig, G. W. *Phys. Rev.* **1961**, *124*, 1083.
(5) Verma, A. R.; Krishna, P. *Polymorphism and Polytypism in Crystals*; Wiley: New York, 1966.
(6) Bailey, S. W.; Frank-Kamenetskii, V. A.; Goldstaub, S.; Kato, A.; Pabst, A.; Taylor, H. F. W.; Fleischer, M.; Wilson, A. J. C. *Acta Crystallogr.* **1984**, *A40*, 499.

0897-4756/91/2803-0332$02.50/0